Thermal boundary resistance between liquid helium and silver sinter at low temperatures

Vonken, A.P.J.; Riese, D.; Roobol, L.P.; König, R.; Pobell, F.

DOI
10.1007/BF00754629

Publication date
1996

Document Version
Final published version

Published in
Journal of Low Temperature Physics

Journal of Low Temperature Physics, Vol. 105, Nos. 1/2, 1996

Thermal Boundary Resistance Between Liquid Helium and Silver Sinter at Low Temperatures

A. P. J. Voncken,* D. Riese, L. P. Roobol,† R. König, and F. Pobell**,[1]**

† *Dept. Phys., Royal Holloway, Univ. of London, Egham, Surrey TW20 0EX, UK*
* *Dept. Phys., Univ. of Nottingham, University Park, Nottingham NG7 2RD, UK*
** *Physikalisches Institut, Univ. Bayreuth, D-95440 Bayreuth, Germany*

(Received April 29, 1996; revised July 8, 1996)

We present measurements of the thermal coupling between Ag sinter (nominal grain size $\approx 700\,\text{Å}$) and superfluid ^{3}He-B at $p = 0.3$, 10, and 20 bar as well as a phase-separated ^{3}He-^{4}He mixture at $p = 0.5$ bar in the sub-millikelvin regime. In order to analyze the data of the pure ^{3}He-B sample with respect to different contributions to the thermal resistance, a one-dimensional model for the heat flow in the sinter is presented. As a result it is shown that the thermal conductivity of the liquid in the sinter has to be taken into account to extract the temperature and pressure dependence of the boundary resistance in the confining geometry of the sinter. Depending on the value of this thermal conductivity, a boundary resistance proportional to T^{-2} or T^{-3} is found. Moreover, it is shown that a pressure dependence of the boundary resistance might be explained by a pressure dependence of the thermal conductivity of the liquid in the sinter. The data on the phase-separated mixture are equally well described by a T^{-2}- and a T^{-3}-dependence of the boundary resistance. We point out that a common problem in most measurements of the Kapitza resistance performed so far is the small temperature interval investigated, which usually does not allow a definite conclusion concerning the temperature dependence.

1. INTRODUCTION

The large difference in the acoustic impedances of liquid helium and a metal is responsible for the existence of a substantial temperature difference ΔT at the liquid/solid interface in the presence of a heat flow $\dot{Q}$ across the boundary. The ratio of this temperature difference and the corresponding heat flow is defined as the thermal boundary resistance across this interface, known as Kapitza-resistance R_K[2]

$$R_K = \frac{\Delta T}{\dot{Q}} \tag{1}$$

0022-2291/96/1000-0093$09.50/0

In general, R_K is a function of temperature. Assuming that only phonons contribute to the energy exchange between both materials, the temperature dependence of the Kapitza resistance at a helium/metal interface is proportional to T^{-3}, as was first predicted in the so-called acoustic mismatch theory by Khalatnikov.[3] Obviously, if heat transfer via phonons were the only possible mechanism for heat transfer across a liquid helium/solid interface, the strong temperature dependence of R_K would not allow the cooling of liquid helium into the lower millikelvin or even microkelvin temperature range.

The most important technical means to reduce the large temperature difference at the interface is the use of fine metal powder sinter. With typical powder grain sizes of about 1000 Å, large specific surface areas of the order of 1 to 2 m^2/g for Cu and Ag powder and up to 20 m^2/g for Pt powder can be achieved.[4] Heat exchangers with surface areas of several hundreds of m^2 are commonly used in low temperature experiments, thus improving the thermal contact between the liquid and the solid enormously. The efficiency of this type of thermal contact strongly depends on the way the metal powder is treated thermally and mechanically. Important to mention are: the different "recipes" of pre-sintering and sintering of the powder, the variation of its packing fraction due to the applied pressure, and the content of impurities in the powder (especially hydrogen, oxygen, and magnetic impurities).[4] In a number of investigations[5-10] several properties of Cu and Ag sinters, like packing fraction and the effect of heat treatment, have been characterized. Together with Pt these metals are the most commonly used materials for sinter sponges in low temperature experiments on liquid helium.

The use of heat exchangers made of ultrafine particles pressed to sinter sponges directly affects the physics of the energy transfer in the sinter volume. In the last decades a number of experiments performed at temperatures below about 10 mK show deviations from the acoustic mismatch theory concerning the magnitude as well as the temperature dependence of R_K. These experiments report a much better thermal coupling between liquid helium and the sinter heat exchanger than predicted by the acoustic mismatch theory. Obviously, the acoustic mismatch theory is no longer adequate at these low temperatures and in confining geometries. Experimental results for $^3He^4$-He mixtures, for instance, indicate that the temperature dependence of the boundary resistance behaves as T^{-2},[11-16] and in ^3He even $R_K \propto T^{-1}$ has been observed.[11,17-19] This strongly improved thermal contact at very low temperatures is commonly attributed to two different origins: firstly, the existence of new vibrational modes in the sinter (soft-phonon modes) due to the finite size of the sinter particles,[6,20,21] and secondly, the observation of a magnetic channel for heat

transfer.[13, 19] A review on the experimental and theoretical aspects of the thermal boundary resistance between sintered metal powders and ^{3}He and ^{3}He-^{4}He mixtures is given in Ref. 22. A large collection of experimental data on this subject can be found in the earlier review of Harrison.[23]

The Kapitza resistance is commonly measured by applying heat to the liquid and simultaneously monitoring the temperatures of the liquid and the cell body. Usually the data are then directly analyzed according to the definition of R_K as given by Eq. (1). This analysis, however, is a strong simplification of the actual situation, as it deals only with the existence of one type of thermal resistance between the helium and the sinter body and hence does not take into account thermal resistances of the liquid in the sinter pores and of the sinter sponge. There are only few experiments on the boundary resistance discussing the impact of these additional thermal resistances but even then simplifying assumptions are introduced in the analysis. The observation of Cousins *et al.*[24] of a length scale that is involved in the heat flow between the sinter and a saturated mixture clearly points out the importance of these additional thermal resistances. Their experimental results, however, suggest $R_K \propto T^{-3}$ at low temperatures which is in disagreement with most of the recent measurements as already mentioned above. Even more pronounced differences concerning the thermal boundary resistance between a sinter body and superfluid ^{3}He have been reported. Ahonen *et al.*[18] observed $R_K \propto T^{-1}$ in ^{3}He at $0.4\,\text{mK} < T < 10\,\text{mK}$, without a change in the temperature dependence of R_K at the superfluid transition, whereas an exponential temperature dependence of the boundary resistance of superfluid ^{3}He was observed by Parpia[25] and by Castelijns *et al.*[26]

The motivation for our work was to study the common difficulties in the determination of the temperature dependence of the boundary resistance which led to different results obtained by different groups, and to search for possible ways of resolving these problems. In this paper, we report on experimental data of the boundary resistance between a silver sinter and superfluid ^{3}He at $p = 0.3$ bar, 10 bar, and 20 bar at temperatures between $0.15T_c$ and $0.5T_c$ and the analysis of these data with a heat flow model. Here, T_c is the superfluid transition temperature of ^{3}He-B which increases with pressure from $T_c = 0.929$ mK at $p = 0$ bar to $T_c = 1.83$ mK at $p = 10$ bar and $T_c = 2.24$ mK at $p = 20$ bar.[28] In addition, we have performed measurements of the thermal boundary resistance between a saturated ^{3}He-^{4}He mixture and silver sinter. After a short description of the experimental setup in the next section, our data are presented in section 3 where they are analyzed in the usual way, i.e., using only the definition of the Kapitza resistance (Eq. 1). In section 4, a one-dimensional model for the heat flow in a sinter slab is presented. Then in section 5, our data are

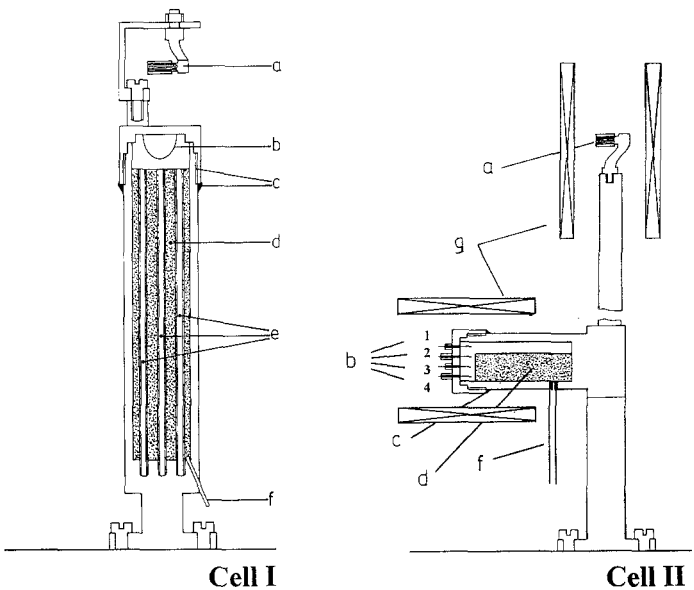

Fig. 1. Schematic view of the experimental cells. (a) Pt-NMR thermometer, (b) vibrating wires, (c) Stycast sealing (2850 FT), (d) Ag sinter heat exchanger, (e) silver posts and channels, (f) filling capillaries, (g) field coils. The horizontal arrangement of the vibrating wires in cell II enables to detect the position of the phase boundary of a saturated phase-separated mixture (see text). In addition, cell II contains a PtW wire as heater in the liquid; it is positioned in the lower part of the cell approximately on the same level as wire no. 3.

analyzed with this model. This implies that now the thermal resistances of the liquid in the sinter pores and of the sinter itself are taken into account. Finally, the results are summarized in section 6.

2. EXPERIMENTAL DETAILS

The boundary resistance measurements were performed in two different experimental cells that were attached to the top flange of our Cu nuclear demagnetization refrigerator.[27] A schematic view of the cells is shown in Fig. 1; a more detailed description of the two cells, which were in the cryostat one at a time, can be found in Ref. 29. Both cells have the same basic design: they consist of cylindrical cell bodies made of pure, annealed silver. Apart from an open space of about 1 cm^3 for several vibrating wires (serving as thermometers, viscometers or heaters) the cells are entirely filled with an Ag sinter sponge.[30] The main difference between the cells is the size of the surface area of the heat exchangers. The larger

cell, in this work referred to as cell I, has a sinter surface area of 110 m^2. This is about one order of magnitude larger than the 12 m^2 surface area of the smaller cell II.

Boundary resistance measurements require the determination of the temperature of the liquid and the temperature of the cell body with high accuracy in order to resolve the temperature difference ΔT between the liquid and the cell body. The sub-millikelvin temperature regime of our measurements requires the use of Pt-NMR thermometers to detect the temperature of the cell bodies. The temperature of the liquid was determined from the damping of the wires vibrating in the liquid.[29, 31, 32] Below the superfluid transition temperature of ^{3}He, the damping of a wire, characterized by the linewidth of its resonance curve, decreases by more than four orders of magnitude, thus providing an extremely sensitive thermometer for the liquid in this temperature regime. In liquid ^{3}He-^{4}He mixtures, however, vibrating wire thermometry is only applicable to about 2 mK. At lower temperatures the mean free path of the ^{3}He quasiparticles is the dominant length scale in the system which leads to a temperature independent linewidth of the resonance curves. In a phase-separated mixture, however, we are able to overcome this problem by immersing the wire into the almost pure ^{3}He phase floating above the saturated mixture. Assuming that the thermal boundary resistance between the two liquid phases is negligible, the wire in the ^{3}He phase provides a sensitive thermometer for *both phases* in the microkelvin temperature range.[29]

Below about $0.15\,T_c$, the damping of the ^{3}He quasiparticles becomes comparable to the intrinsic damping of the wires used in our experiments which therefore determines the lower limit for our temperature measurements. The relatively small magnetic field of maximum 40 mT the vibrating wires are exposed to determines the upper temperature limit in the liquid to $\sim 0.5\,T_c$ as above this temperature the temperature resolution from the damping of the wire is no longer sufficient. Our investigation of the boundary resistance is therefore restricted to 0.15 mK $< T <$ 0.43 mK at $p = 0.3$ bar, 0.43 mK $< T <$ 0.80 mK at $p = 10$ bar and 0.51 mK $< T <$ 1.2 mK at $p = 20$ bar.

In cell II, a PtW wire (2 mm long, $\varnothing$ 20 μm), soldered to superconducting NbTi wires, served as heater in the liquid. This PtW heater was immersed into the liquid at a distance of approximately 10 mm from the cell walls. Additional PtW wires were attached on the outside walls of both cells in order to measure the thermal coupling of the cells to the Cu nuclear refrigerating stage. Knowing the thermal coupling coefficient, the heat leak from the cell to the stage is directly accessible.[29] This so-called intrinsic heat leak $\dot{Q}_{\mathrm{intr}}$ of the *empty* cell turned out to decay slowly with time. The origin of this heat leak was attributed to the ortho-para conversion of

hydrogen in the sinter.[29, 33] With liquid in the cell an extra heat release from the liquid in the sinter becomes noticeable. This heat leak, hereafter referred to as residual heat leak $\dot{Q}_{\text{res}}$, was accurately determined by subtracting the data of the empty cell heat release from the overall heat leak (cell plus liquid), assuming that the heat leaks from different sources behave additively. The residual heat release from a saturated mixture turned out to be much larger than that of pure ^{3}He and decreased from several hundred picowatts to about 15 pW within the first ten days after the mixture was condensed into the cells.[29] Of course, the presence of a non-negligible residual heat leak $\dot{Q}_{\text{res}}$ had to be taken into account in the analysis of the boundary resistance data.

3. RESULTS

The measurements of the boundary resistance between the silver sinter sponge and superfluid ^{3}He were performed in cell II at pressures of $p = 0.3$, 10, and 20 bar. We assume that the temperature dependence of the Kapitza resistance is given by

$$R_K A T^n = r \tag{2}$$

where A is the surface area of the heat exchanger and r is a constant.[34] The value of r can be found by integrating Eq. (2) over a small temperature difference $\Delta T = T_L - T_S$ at the boundary. This gives

$$T_L^{n+1} - T_S^{n+1} = r(n+1)\frac{\dot{Q}}{A} \tag{3}$$

with T_L and T_S the temperatures of the liquid and the solid, respectively. A straight line in a plot of $T_L^{n+1} - T_S^{n+1}$ versus $\dot{Q}$ gives the exponent n and since the value of A is known the coefficient r can be extracted from its slope.

Figure 2 shows our experimental results for the thermal resistance between superfluid ^{3}He and a 700 Å Ag sinter at $p = 0.3$ bar. For simplicity, we only present the data taken at $p = 0.3$ bar which, however, are representative for all other results obtained with superfluid ^{3}He. The three plots correspond to values of $n = 1, 2, 3$, i.e. to different possible temperature dependences of the boundary resistance. The horizontal axis is given by the total heat load, i.e., the sum of the externally applied heating power and the residual heat leak at the time the measurement was performed. An important underlying assumption in our analysis is that the total heating power supplied by the small PtW wire is indeed completely transferred into the liquid. The solid lines in Figs. 2a, b, and c are linear fits to the data.

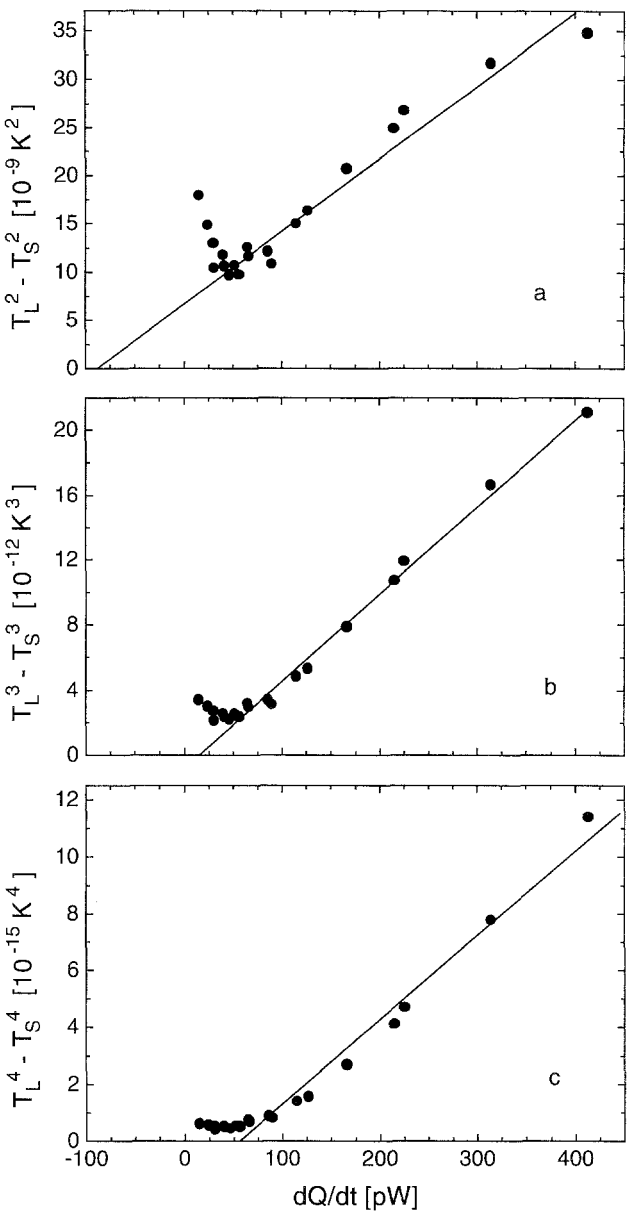

Fig. 2. $(T_L^{n+1} - T_S^{n+1})$ versus total heat $\dot{Q}$ for ^{3}He-B at $p = 0.3$ bar for (a) $n = 1$, (b) $n = 2$, and (c) $n = 3$ in the temperature range $0.15\,\text{mK} < T < 0.43\,\text{mK}$. The increase or saturation of the data for $\dot{Q} < 50\,\text{pW}$ is due to the insensitivity of the vibrating wires at the lowest temperatures; therefore the data were fitted for $\dot{Q} > 50\,\text{pW}$ only (solid lines).

Obviously, Fig. 2a shows that our experimental data are only poorly described by $R_K \propto 1/T$. This result is in contrast to the observation of Ahonen *et al.*[18] for ^{3}He at zero pressure between 0.4 mK and 10 mK. On the other hand, there is only a small difference between a fit to $R_K \propto T^{-2}$ and $R_K \propto T^{-3}$ as far as the quality of the fit is concerned. However, the independent measurement of the residual heat leak from the liquid provides a second and equally important condition that must be satisfied: since in the figures the total heating power is plotted along the horizontal axis, i.e. the residual heat leak has been taken into account, the intercept of the straight line determined by the fit with the x-axis should be zero. Table I shows the important quantities extracted from the fits. The quality of the fit is expressed by the correlation coefficient C, and $\dot{Q}_r$ denotes the intercept of the straight lines with the horizontal axis. At all three pressures, the quality of the fit as well as the argument concerning the intercept favour a T^{-2}-dependence of the boundary resistance. The magnitude of the thermal resistance extracted from the slope of the plots with $n=2$ is $R_K A T^2 = 0.19$ (0.48, 0.67) K^{3}m^2/W at $p = 0.3$ (10, 20) bar, respectively.

The fact that it is very difficult to extract a unique temperature dependence of the boundary resistance is even more pronounced for our data on a phase-separated saturated ^{3}He-^{4}He mixture. Figs. 3a, b show the data of measurements (using a PtW wire as heater of the liquid) with the phase boundary of a phase-separated mixture being located *within* the sinter heat exchanger in cell II. In this cell, the horizontal arrangement of the vibrating wires (see Fig. 1) enables us to determine the position of the phase boundary with an accuracy of about 2.5 mm which is the distance between the planes of the loops of two wires. The data presented in Fig. 3 were taken with the phase boundary positioned between the wires labeled 1 and 2 in Fig.1, and therefore, as the position of the lower wire (no. 2) is just below the horizontal surface of the sinter body, the ^{3}He phase could have been in contact to about 1 m^2 of the sinter surface area.

TABLE I

The Quality of the Fits to the Data Obtained with Superfluid ^{3}He, Expressed by the Correlation Coefficient C, and the Intercept $\dot{Q}_r$ of the Straight Lines with the X-axis, See Fig. 2

p [bar]		$n=1$	$n=2$	$n=3$
0.3	C	0.97867	0.9964	0.98886
	$\dot{Q}_r$ [nW]	−0.09	0.02	0.06
10	C	0.96198	0.99766	0.99497
	$\dot{Q}_r$ [nW]	−0.47	−0.08	0.09
20	C	0.93556	0.99917	0.97246
	$\dot{Q}_r$ [nW]	−0.78	0.05	0.33

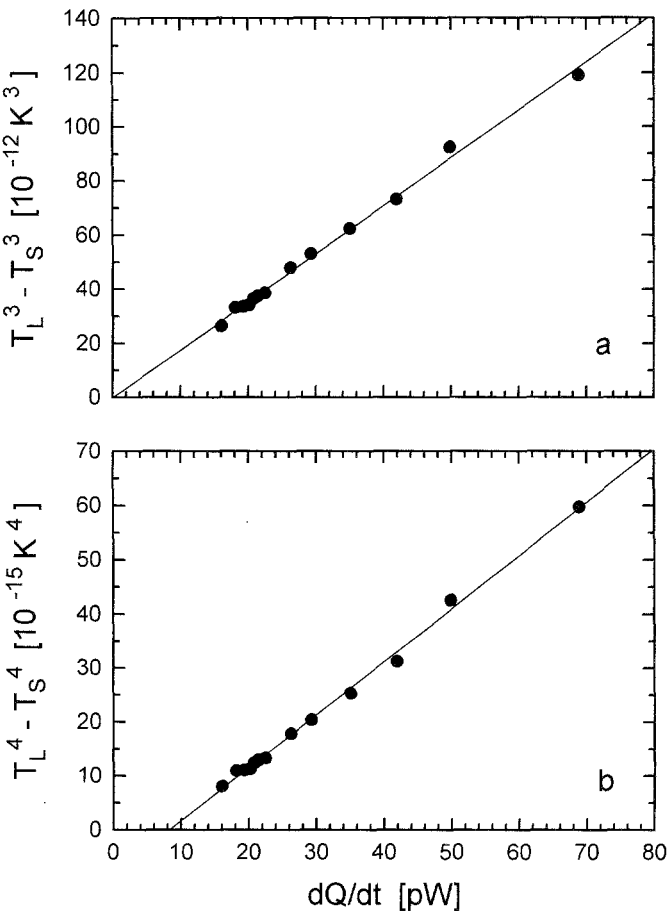

Fig. 3. $(T_L^{n+1} - T_S^{n+1})$ versus total heat $\dot{Q}$ for a phase-separated mixture with the phase boundary being located within the sinter. The temperature range was 0.30 mK $< T <$ 0.52 mK. Assuming that the resistance across the phase boundary can be neglected, the measured resistance is essentially the parallel resistance between the sinter and both liquid phases. The straight lines are given by $AR_K T^2 = 6.5\ \mathrm{m^2K^3/W}$ (a) and $AR_K T^3 = 0.0029\ \mathrm{m^2K^4/W}$ (b), respectively.

There is no difference between a fit to $R_K \propto T^{-2}$ and $R_K \propto T^{-3}$ as far as the quality of the fit is concerned. Again, the argument concerning the intercept favours a T^{-2}-dependence of R_K. However, the small difference between the two cases does not allow us to extract a definite temperature dependence. The magnitude of the boundary resistance shown in Figs. 3a, b suggests that in case both phases of a phase-separated mixture are in contact

with the sinter the parallel resistance is significantly smaller compared to the R_K of the mixture only (see below and Fig. 4).

Figure 4 shows a plot of $T_L^{n+1} - T_S^{n+1}$ versus $\dot{Q}$ for $n=2$ and 3 for a phase-separated mixture at $p=0.5$ bar in cell I. The importance of this plot is the fact that the x-axis is given by the residual heat leak of the mixture only; that is, no heat was applied with a wire heater for this measurement.

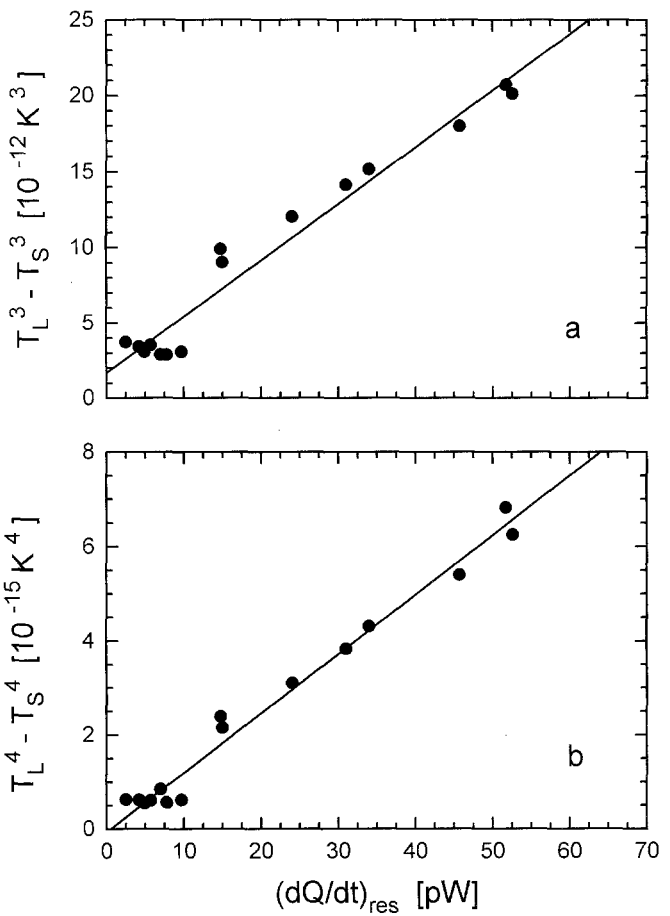

Fig. 4. $(T_L^{n+1} - T_S^{n+1})$ versus residual heat leak for a phase-separated mixture with $n=2$ (a) and $n=3$ (b) in the temperature range $0.16\ \text{mK} < T < 0.35\ \text{mK}$. The scatter of the data at $\dot{Q}_{res} < 10$ pW is due to the insensitivity of the Ta wire at the lowest temperatures. The straight lines are linear fits to the data at $\dot{Q}_{res} > 7$ pW and are given by $AR_K T^2 = 14\ \text{m}^2\text{K}^3/\text{W}$ (Fig. a) and $AR_K T^3 = 0.0035\ \text{m}^2\text{K}^4/\text{W}$ (Fig. b), respectively.

The measurements were taken at different times after the mixture was condensed into the cell, thus exploiting the fact that the residual heat leak of the mixture decayed slowly with time. In this case, the often discussed problem whether heating a wire in the liquid indeed completely transfers the applied heat into the liquid is no longer relevant. As a consequence the linear fit in a plot of $T_L^{n+1} - T_S^{n+1}$ versus $\dot{Q}_{\text{res}}$ has to cross the origin within experimental error. This argument as well as the quality of the fit favours a T^{-3}-dependence of the boundary resistance, as can be seen from Figs. 4a, b. However, the difference between a fit to $R_K \propto T^{-2}$ and $R_K \propto T^{-3}$ is so small that no definite conclusion concerning the temperature dependence can be drawn.

The problems in analyzing data of the thermal boundary resistance mainly result from two origins that are shared in most other experiments on the boundary resistance so far: firstly, because of the relatively small temperature range of boundary resistance experiments, the temperature dependence of R_K can not clearly be determined. In our case, the small temperature range accessible by the vibrating wire thermometry does not allow an unambiguous distinction between a T^{-3}- and T^{-2}-dependence of the boundary resistance. Secondly, in using the definition of the Kapitza resistance (Eq. 1) for the analysis of experimental data, one neglects the thermal resistances within the sinter and within the liquid in the sinter. For the latter problem, we tried to analyze our data obtained with ^{3}He on the basis of a one-dimensional model for the heat exchange in the sinter, taking the finite thermal conductivity of the liquid inside a sinter and of the sinter itself into account. This model is an extension of the models discussed by Krusius *et al.*[5] and Cousins *et al.*[24] which may be considered as limiting cases of the model presented below.

4. A ONE-DIMENSIONAL MODEL FOR THE HEAT FLOW IN A SINTERED HEAT EXCHANGER

The finite thermal conductivities of the sinter sponge, κ_S, and of the liquid in the sinter pores, κ_l, result in temperature gradients in the sinter volume, that, especially at low temperatures, might become important in the analysis of the thermal coupling between liquid helium and a sintered heat exchanger. In the model presented in this section the possible existence of a parallel channel for heat transfer via soft-phonons as well as the dependence of the boundary resistance on an externally applied magnetic field are neglected. The magnetic field for the viscometer applied during our measurements was 40 mT near the wires and significantly less over the sinter region.

In the above discussed analysis of the data according to Eq. (3), the experimental situation is simplified to a single liquid-solid interface with an

exchange area A and an *effective* boundary resistance R_K. This effective boundary resistance contains the thermal resistances of the sinter sponge and of the liquid in the sinter. In order to extract the temperature dependence and the magnitude of the real boundary resistance in the restricted geometry of the sinter, we now consider the heat transport in a homogeneous sinter slab of thickness ℓ and cross-sectional area A_c (Fig. 5). Although it is still a substantial simplification of the real experimental situation, this approach should be more appropriate for the analysis of the data than the reduction to an interface.

A schematic view of the sinter slab is shown in Fig. 5. The bulk-liquid/sinter interface is located at $x=0$ and the cell wall at $x=\ell$. To derive a local equation for the heat transport of the liquid in the sinter and of the sinter sponge itself we apply Eq. (3) to a slice of sinter with thickness $\Delta x \ll \ell$ at position x, assuming the existence of a power law for $R_K(T)$. This results in $\Delta \dot{Q}_l = \Delta A[T_l^{n+1}(x) - T_s^{n+1}(x)]/(n+1)\,r$, where $\Delta \dot{Q}_l$ denotes the heat transferred from the liquid to the sinter in the slice, ΔA the surface area of the slice, and $T_{l,s}(x)$ are the temperatures of the liquid in the sinter (subscript l) and of the sinter itself (subscript s) at position x. For a homogeneous sinter we have $\Delta A = A\Delta x/\ell$. Letting $\Delta x \to 0$ then yields

$$\frac{\partial}{\partial x}\dot{Q}_s = -\frac{\partial}{\partial x}\dot{Q}_l = \frac{A}{(n+1)\,r\ell}(T_l^{n+1}(x) - T_s^{n+1}(x)) \tag{4}$$

where $\dot{Q}_{l,s}$ denotes the heat flow in the liquid and in the sinter, respectively. The corresponding differential equations for the spatially varying temperatures

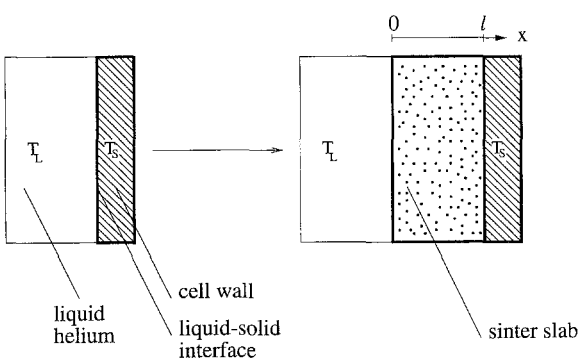

Fig. 5. Schematic view of the sinter slab (right sketch) used in the model discussed in this work, in comparison with the situation used in the conventional analysis of Kapitza resistance data (left sketch).

$T_{l,s}(x)$ can be derived from Eq. (4) by simply inserting the relations

$$\dot{Q}_s = -A_c \kappa_s \frac{\partial}{\partial x} T_s \tag{5}$$

$$\dot{Q}_l = -A_c \kappa_l \frac{\partial}{\partial x} T_l \tag{6}$$

which define the thermal conductivities $\kappa_{l,s}$ with respect to the cross-sectional area A_c of the sinter slab.

At this stage, one has to make an assumption concerning the temperature dependences of the thermal conductivities $\kappa_{l,s}$. In the case of κ_s we can assume a linear temperature dependence, i.e $\kappa_s = k_s T_s$, since in a metal at low temperatures heat is carried mainly by the conduction electrons. The magnitude of the constant factor k_s follows from the Wiedemann–Franz law, which gives for this type of sinter $k_s \simeq 0.15$ W/K^{2}m.[6, 7]

The estimation of the thermal conductivity of the liquid in the sinter is a more difficult matter. It was shown by Betts *et al.*[35] experimentally that the thermal conductivity of normal fluid ^{3}He in the confining geometry of Vycor glass depends linearly on temperature, in contrast to $\kappa_l \propto 1/T$ for the bulk Fermi liquid. However, there are no data available for ^{3}He in a sintered heat exchanger. Therefore, one has to resort to some theoretical model as far as the magnitude of κ_l is concerned.

We have modelled the sinter as consisting of spherical pores with a typical diameter of 1000 Å[36] which are connected by narrow channels. In the pores, where the dimensions are larger than the coherence length of the Cooper pairs ($\xi_0 \simeq$ 750 Å at $p = 0$ bar), the liquid undergoes a superfluid transition at sufficiently low temperatures. However, in the narrow channels between the pores, where the dimensions might be much smaller than the coherence length, the liquid is assumed to stay in its normal state; thus we may apply Fermi-liquid theory.[39] As the mean spatial extension for the normal fluid in a channel we take the coherence length at $T = 0$, which decreases with increasing pressure. We now assume that the thermal resistance of the liquid in the sinter is dominated by that of the normal fluid part in the narrow channels between the sinter pores. Since the dimensions inside a channel are much smaller than the quasiparticle mean free path at the temperatures investigated here, the thermal conductivity of this normal component is taken to be proportional to temperature, i.e., $\kappa_l = k_l T_l$.

The magnitude of k_l can be estimated using this model, and since the coherence length is pressure dependent, k_l also depends on pressure. The presence of a superfluid component of the liquid leads to corrections in the thermal conductivity compared to a sinter completely filled with normal

fluid. We estimate $k_l = 0.4$, 0.1, and 0.05 W/K^{2}m at pressures $p = 0.3$, 10 and 20 bar, respectively; these values may be considered as upper limits for the thermal conductivity of the liquid in the sinter. However, one should bear in mind that the real situation in the sinter will be much more complicated than assumed in this model. The values for the thermal conductivity of the liquid in the sinter should therefore be regarded as rough estimates only.

With the linear temperature dependences of κ_s and κ_l, we get

$$\frac{1}{2}\frac{\partial^2 T_{l,s}^2(x)}{\partial x^2} = \pm\frac{A}{(n+1)\,\ell r A_c k_{l,s}}\left(T_l^{n+1}(x) - T_s^{n+1}(x)\right) \tag{7}$$

where the positive (negative) sign corresponds to the equation describing the temperature variation in the liquid (sinter). For $n = 1$, i.e., $R_K \propto 1/T$, Eq. (7) has a simple analytical solution. For $n \neq 1$, this set of coupled non-linear differential equations can only be solved numerically. In the limiting case of $k_l \gg k_s$ the analytical solution with $n = 1$ reduces to the model used by Krusius *et al.*[5] The approach of Cousins *et al.*[24] corresponds to the analytical solution in the opposite case, i.e., $k_l \ll k_s$.

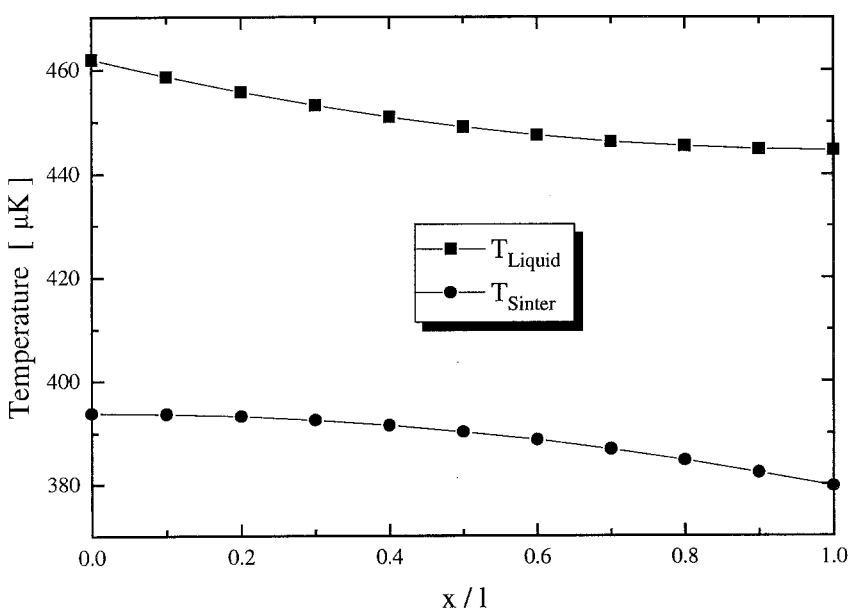

Fig. 6. Numerically calculated temperature profiles in a sinter slab with a cross-sectional area of 4.2 cm^2 and of 2.5 mm thickness. The parameters are: $n = 2$, $k_s = 0.15$ W/K^{2}m, $k_l = 0.1$ W/K^{2}m and $AR_K T^2 = 0.48$ K^{3}m^2/W.

Moreover, with $n=1$ a relation between the bulk liquid temperature $T_l(x=0)$, the cell wall temperature $T_s(x=\ell)$, and the total heat release, $\dot{Q}=\dot{Q}_l+\dot{Q}_s$, can be found:

$$T_l^2(0)-T_s^2(\ell)=\frac{2\dot{Q}r}{A}\left(\frac{\gamma}{\sinh(\gamma)}\right)\left(\frac{2+\gamma\sinh(\gamma)+\mathcal{K}\cosh(\gamma)}{2+\mathcal{K}}\right) \tag{8}$$

where $\gamma^2=(\ell A/r)(1/k_l+1/k_s)$ and $\mathcal{K}=(k_s/k_l+k_l/k_s)$. Note that for $n=1$, $(T_l^2(0)-T_s^2(\ell))$ is proportional to $\dot{Q}$, irrespective of the values of k_l and k_s. In the case where $\gamma\ll 1$, relation (8) reduces to $T_l^2(0)-T_s^2(\ell)=2\dot{Q}r/A+O(\gamma^2)$ which is equal (to order γ) to Eq. (3) for $n=1$.

Figure 6 shows a typical result of the calculated temperature profiles in the sinter obtained by solving Eqs. (7) numerically. Details of the input parameters are given in the figure caption. Important to note here is that the temperature variations in the liquid and in the sinter are of the same order of magnitude as the difference between the bulk liquid and cell wall temperatures. This points out the importance of the extra thermal resistances in the sinter volume compared to the Kapitza resistance. In the next section, the data of the thermal resistance measurements in superfluid ^{3}He-B at $p=0.3$, 10, and 20 bar are analyzed via this model for the heat flow in a sinter slab.

5. DATA ANALYSIS USING THE HEAT FLOW MODEL

Before we can analyze our data in terms of the heat flow model presented above, we need to determine the parameters A_c and ℓ for the actual sinter geometry. In cell II we had a bulk liquid/sinter surface area of 4.2 cm^2. The estimated "average" distance through the sinter from this bulk liquid/sinter interface to the cell wall is about 2.5 mm. The product $A_c\cdot\ell$ is remarkably close to the actual sinter volume of 1 cm^3, which justifies the modelling of our sinter geometry by a slab with area $A_c=4.2$ cm^2 and thickness $\ell=2.5$ mm.

We have analyzed the experimental data in the following way:

1. For a given n, a first estimate for r is chosen. The temperature profiles in the sinter are then calculated by solving Eqs. (7) numerically, with the experimental quantities $\dot{Q}$ and T_S determining the boundary conditions. The calculation is performed for all data points, that is, for all sets of $\dot{Q}$ and T_S.
2. The calculated liquid temperature $T_l(x=0)$ is compared to the measured liquid temperature T_L for all data points.

3. The value of r is varied to minimize the relative deviation $\Delta T_L/T_L \equiv (T_l(0) - T_L)/T_L$.
4. The procedure is repeated for a new value of n.

Note that the only fitting parameter of the model for given n is the coefficient r of the boundary resistance. All other parameters have been estimated independently from the geometry of the experimental cell or from physical arguments.

A typical result of a fit is shown in Fig. 7. On the vertical axis $\Delta T_L/T_L \equiv (T_l(0) - T_L)/T_L$ is plotted for the data taken at $p = 10$ bar. The three sets shown correspond to $n = 1, 2$, and 3, i.e., different temperature dependences of the boundary resistance. From this figure we see that the fit with $n = 1$, i.e. with a Kapitza resistance proportional to $1/T$, gives the largest deviation of the calculated liquid temperature from the measured liquid temperature. Furthermore, there is a preference for a T^{-3}-temperature dependence of R_K for this particular choice of k_l and k_s. This is in contrast to the results obtained in section 3, where we had neglected the temperature gradients in the liquid in the sinter and in the sinter itself. However, due to the small temperature range resulting from the limitations of the vibrating

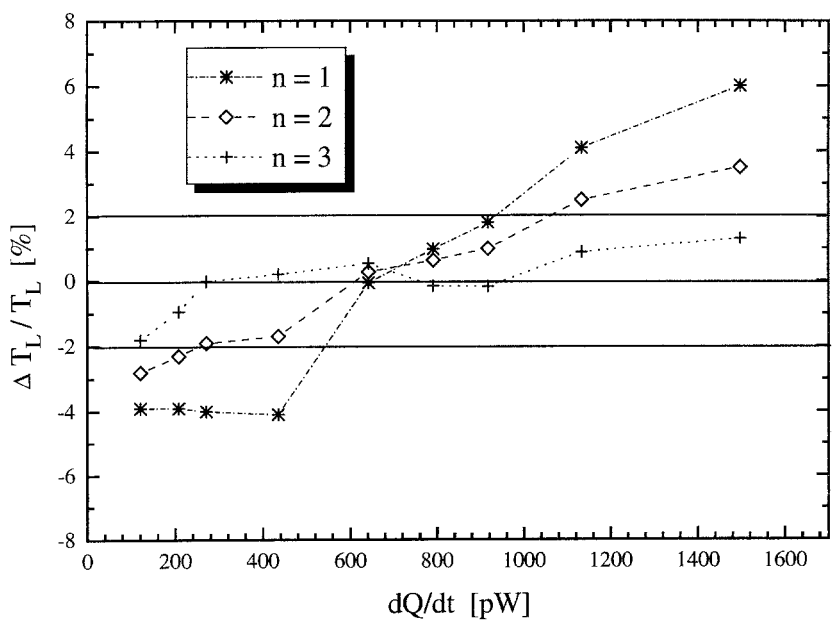

Fig. 7. Typical plot of the relative difference between calculated and measured liquid temperature versus heat input in the liquid at $p = 10$ bar. The data correspond to Kapitza resistances proportional to $1/T^n$ with $n = 1$ (stars), $n = 2$ ($\diamond$), and $n = 3$ ($+$).

TABLE II

The Dependence of the Coefficient r of the Boundary Resistance (see Eq. (3)) and the Corresponding Value of ε (Average Values of $|\Delta T_L/T_L|$) on Pressure p, Thermal Conductivity k_l of the Liquid, and the Exponent n of the Temperature Dependence of R_K. The Data Presented Were Calculated Using $k_s = 0.15$ W/K^{2}m, $l = 2.5$ mm and $A_c = 4.2$ cm^2

		0.3 bar		10 bar		20 bar	
k_l [W/K^{2}m]	n	r [m^{2}K^{n+1}/W]	ε [%]	r	ε	r	ε
	1	571	2.8	683	3.3	800	2.4
0.4	2	$137 \cdot 10^{-3}$	1.2	$366 \cdot 10^{-3}$	1.4	$514 \cdot 10^{-3}$	0.6
	3	$28.6 \cdot 10^{-6}$	2.0	$194 \cdot 10^{-6}$	0.7	$320 \cdot 10^{-6}$	1.4
	1	400	2.8	491	3.2	629	2.4
0.1	2	$91.0 \cdot 10^{-3}$	1.4	$274 \cdot 10^{-3}$	1.8	$422 \cdot 10^{-3}$	1.1
	3	$19.4 \cdot 10^{-6}$	1.2	$143 \cdot 10^{-6}$	0.7	$240 \cdot 10^{-6}$	0.6
	1	229	2.9	297	3.2	434	2.4
0.05	2	$57.0 \cdot 10^{-3}$	2.0	$183 \cdot 10^{-3}$	2.3	$286 \cdot 10^{-3}$	1.3
	3	$11.4 \cdot 10^{-6}$	1.1	$88.0 \cdot 10^{-6}$	1.3	$166 \cdot 10^{-6}$	0.4

wire thermometry, even in this improved analysis no definite temperature dependence of the Kapitza resistance can be extracted.

To study the effect of a finite thermal conductivity of the liquid in the sinter on the experimental results we have performed the calculation for all pressures with three different values of the thermal conductivity of the liquid in the sinter. In Table II, the results of these calculations are shown; ε denotes the average value of $|\Delta T_L/T_L|$ over the points at each pressure. The results of these calculations can be summarized as follows:

- A large value of k_l results in a slight preference for a T^{-2}-temperature dependence of R_K. In this case, AR_KT^2 is of the same order of magnitude as that obtained by the previous analysis (section 3).
- Small values of k_l result in a preference for a T^{-3}-law for the temperature dependence of the boundary resistance, in contrast to the simplified analysis given in section 3.
- The assumption of a boundary resistance proportional to T^{-1} gives the largest deviation in all cases.
- For given n and k_l, AR_KT^n increases with pressure, which is in accordance with the results obtained by the conventional analysis (section 3) and by Osheroff and Richardson in normal fluid ^{3}He.[19] However, the apparent pressure dependence of the boundary resistance can always be compensated in case k_l strongly decreases with pressure. For $n = 1$, for example, values of k_l of 0.4, 0.1 and

0.05 W/K^{2}m at pressures $p = 0.3$, 10 and 20 bar lead to a decrease of the boundary resistance with pressure. This result shows the importance of the thermal conductivity of the liquid in the sinter for the determination of the pressure dependence of R_K.

6. SUMMARY AND CONCLUSIONS

This work shows the difficulties that are involved in analyzing data on the thermal coupling of liquid helium to a metal powder heat exchanger. We point out the importance of the extra thermal resistances of the liquid in the sinter and of the sinter itself, that, especially at very low temperatures, should be accounted for in the analysis. An analysis using a one-dimensional model for the heat flows in the sinter shows that the conclusions drawn from the data concerning the temperature and pressure dependences of the boundary resistance depend on the properties of the liquid in the sinter and of the sinter itself. As no data of the thermal conductivity of the liquid in the sinter pores are available at present, we have investigated the impact of this extra thermal resistance on the analysis using different numerical values for the thermal conductivity of ^{3}He in the sinter. It is interesting to note that for superfluid ^{3}He-B the analysis with a model that takes into account the thermal resistance in the sinter leads to a boundary resistance which is best described by a $1/T^3$ temperature dependence for small values of the thermal conductivity of the liquid. This is in contrast to the conventional analysis of the data using Eq. (1), where a $R_K \propto 1/T^2$ is favoured. However, both the conventional analysis as well as the extended analysis yield a $1/T$-dependence of R_K as the most unlikely case. The analysis on the phase-separated mixtures also does not resolve a unique temperature dependence for R_K. Again a boundary resistance $\propto 1/T^2$ or $1/T^3$ fits equally well to the data.

The difference between the results obtained in various experiments with superfluid ^{3}He might be due to the significant differences in the sinter geometry; clearly this is a factor in reported boundary resistance data that needs more attention. Moreover, in most investigations, the temperature range of the measurements seems to be too small to allow an accurate determination of the temperature dependence for R_K.

Furthermore, our analysis shows that the absolute value of the boundary resistance for ^{3}He-B apparently increases with pressure if one applies the definition of the Kapitza resistance directly. However, this result might be explained by assuming that the *thermal conductivity* of the liquid in the sinter pores decreases with pressure. With these points in mind, it seems that experimental data on the thermal conductivity of liquid helium in the sinter pores are of prime importance for a more conclusive analysis of this type of thermal boundary resistance measurements.

ACKNOWLEDGMENTS

We gratefully acknowledge the contributions of A. Betat. This work was supported by the Deutsche Forschungsgemeinschaft by grant Po 88/18 and by the Graduiertenkolleg Po 88/13, as well as the "Human Capital and Mobility: Large Scale Facility" program of the EC.

REFERENCES

1. New address: Forschungszentrum Rossendorf, D-01314 Dresden, Germany.
2. P. L. Kapitza, *Zh. Eksp. & Teor. Fiz.* **11**, 1 (1941). [*J. Phys. (Russ.)* 4 (181)].
3. I. M. Khalatnikov, *Zh. Eksp. & Teor. Fiz.* **22**, 687 (1952).
4. F. Pobell, Matter and Methods at Low Temperatures, Springer Verlag, Berlin, Heidelberg, 1st ed. 1992, 2nd ed. 1996.
5. M. Krusius, D. N. Paulson, and J. C. Wheatley, *Cryogenics* **18**, 649 (1978).
6. R. J. Robertson. F. Guillon and J. P. Harrison, *Can. J. Phys.* **61**, 164 (1983).
7. P. A. Busch, S. P. Cheston, and D. S. Greywall, *Cryogenics* **24**, 445 (1984).
8. H. Franco, J. Bossy, and H. Godfrin, *Cryogenics* **24**, 477 (1984).
9. K. Rogacki, M. Kubota, E. G. Syskakis, R. M. Mueller, and F. Pobell, *J. Low Temp. Phys.* **59**, 397 (1985).
10. W. Itoh, A. Sawada, A. Shinozaki, and Y. Inida, *Cryogenics* **31**, 453 (1991).
11. G. Frossati, *J. de Phys. (France)* **C6**, 1578 (1978).
12. D. D. Osheroff and L. R. Corruccini, *Phys. Lett.* **82A**, 38 (1981).
13. D. Ritchie, J. Saunders, and D. F. Brewer, Proc. of 17th Int. Conf. on Low Temp. Phys.; U. Eckern, A. Schmid, W. Weber, and H. Wühl (eds.), Elsevier Science Publishers B.V., p. 743 (1984).
14. G. H. Oh, M. Nakagawa, H. Akimoto, O. Ishikawa, T. Hata, and T. Kodama, *Physica* **B165** & **166**, 527 (1990).
15. G. H. Oh, Y. Ishimoto, T. Kawae, M. Nakagawa, O. Ishikawa, T. Hata, T. Kodama, and S. Ikehata, *J. Low Temp. Phys.* **95**, 525 (1994).
16. H. Ishimoto, H. Fukuyama, N. Nishida, Y. Miura, Y. Takano, T. Fukuda, T. Tazaki, and S. Ogawa, *J. Low Temp. Phys.* **77**, 133 (1989).
17. O. Avenel, M. P. Berglund, R. G. Gylling, N. E. Phillips, A. Vetleseter, and M. Vuorio, *Phys. Rev. Lett.* **31**, 76 (1973).
18. A. I. Ahonen, O. V. Lounasmaa, and M. C. Veuro, *J. de Phys. (France)* **C6**, 265 (1978).
19. D. D. Osheroff and R. C. Richardson, *Phys. Rev. Lett.* **54**, 1178 (1985).
20. A. R. Rutherford, J. P. Harrison, and M. J. Stott, *J. Low Temp. Phys.* **55**, 157 (1984).
21. M. C. Maliepaard, J. H. Page, J. P. Harrison, and R. J. Stubbs, *Phys. Rev.* **B 32**, 6261 (1985).
22. T. Nakayama, Prog. in Low Temp. Phys., D. F. Brewer (ed.), Vol. XII, p. 115 (1989), Elsevier Science Publishers B.V.
23. J. P. Harrison, *J. Low Temp. Phys.* **37**, 467 (1979).
24. D. J. Cousins, S. N. Fisher, A. M. Guénault, G. R. Pickett, E. N. Smith, and R. P. Turner, *Phys. Rev. Lett.* **73**, 2583 (1994).
25. J. M. Parpia, *Phys. Rev.* **B 32**, 7564 (1985).
26. C. A. M. Castelijns, K. F. Coates, A. M. Guénault, S. G. Mussett, and G. R. Pickett, *Phys. Rev. Lett.* **55**, 2021 (1985).
27. K. Gloos, P. Smeibidl, C. Kennedy, A. Singsaas, P. Sekowski, R. M. Mueller, and F. Pobell, *J. Low Temp. Phys.* **73**, 101 (1988).
28. D. S. Greywall, *Phys. Rev.* **B 33**, 7520 (1986).
29. R. König, A. Betat, and F. Pobell, *J. Low Temp. Phys.* **97**, 311 (1994).
30. Ag sinter: *Inabata Corp., Vacuum Metallurgical Ltd., Japan*, (nominal grain size 700 Å).
31. A. M. Guénault, V. Keith, C. J. Kennedy, S. G. Mussett, and G. R. Pickett, *J. Low Temp. Phys.* **62**, 511 (1986).

32. R. König, P. Esquinazi, and F. Pobell, *J. Low Temp. Phys.* **90**, 55 (1993).
33. R. König, A. Betat, L. P. Roobol, A. Voncken, and F. Pobell, *J. Low Temp. Phys.* **101**, 107 (1995).
34. Although an exponential temperature dependence of the boundary resistance in superfluid ^{3}He is also reported in literature,[25, 26] we restrict the analysis of our data to a power law dependence for R_K. There do exist significant differences between the experiments of Refs. 25 and 26 and our experiment that make a comparison of the results with respect to the temperature dependence of the boundary resistance difficult.—In the experiment of Parpia[25] the boundary resistance between superfluid ^{3}He and a heat exchanger made of *bronze flakes* was determined by relaxation time measurements. However, it is reported in this paper that the data were not taken specifically with a view to exposing the temperature dependence of boundary resistance, and that the results might be affected by systematic errors in thermometry.—In contrast to our experiments where the cells were situated in the low field region on top of the nuclear demagnetization stage, the experimental cell of Castelijns *et al.*[26] constitutes the nuclear stage itself. Therefore, during the course of the experiment only the temperature of the liquid changed whereas the temperature of the cell body remained constant due to the large heat capacity of the cell in the final field of demagnetization. An important assumption in the analysis of their data is that the integrated boundary conductance is a function of the helium temperature only, which is fulfilled under the condition that the temperature of their copper cell is considerably lower than that of the ^{3}He, see Ref. 26. In our experiment, heat supplied to the liquid always led to a significant increase in the cell temperature, too, due to the thermal resistance between the cell bodies and the nuclear stage.
35. D. S. Betts, D. F. Brewer, and R. S. Hamilton, *J. Low Temp. Phys.* **14**, 331 (1974).
36. The size of the sinter pores is estimated using the model suggested by Robertson *et al.*[6] The value of the pore size of about 1000 Å is confirmed in specific heat measurements of liquid ^{3}He in a cell entirely filled with Ag sinter which was pressed almost identically as the sinters in cells I and II.[37, 38] The inaccuracy in the determination of the pore size was taken into account in our analysis by calculating the coefficient r of the boundary resistance for *all* thermal conductivities k_l and pressures p.
37. R. Schrenk, R. König, and F. Pobell, *Phys. Rev. Lett.* **76**, 2945 (1996).
38. R. Schrenk and R. König, to be published.
39. The existence of normal fluid ^{3}He in the pores or interconnecting channels of an Ag sinter at $T < T_c$ is confirmed in specific heat measurements in a cell which is completely filled with the sinter; i.e. which has no open space for the liquid, see Ref. 38.